Effect of Silica Nano-Particles on the Transport Behavior of Supercritical CO_2 in Fractured Repositories

Behdad Aminzadeh, Hassan Dehghanpour, Matt Roberts, David DiCarlo, Chun Huh, and Steven Bryant
Department of Petroleum and Geosystems Engineering, The University of Texas at Austin

Contact: behdad.a@mail.utexas.edu

This material is based upon work supported as part of the Center for Frontiers of Subsurface Energy Security, an Energy Frontier Research Center funded by the U.S. Department of Energy, Office of Science, Office of Basic Energy Sciences under Award Number DE-SC00

Introduction

Carbon capture and sequestration (CCS) in the earth's subsurface can potentially offset global CO_2 emissions derived from the combustion of fossil fuels.

Research and development of CCS technology encompasses a wide range of issues to investigate collection of CO_2 from emission streams, transport of CO_2, injection into deep geological environments, and tracking the long-term fate of CO_2 in the subsurface.

Even with the large physical separation between storage reservoirs and surface environments, there remains concern that CO_2 stored in reservoirs may eventually leak back to the surface through abandoned wells or along geological features such as faults.

Leakage would reduce the effectiveness of CCS, possibly lead to human health and ecological impacts at the ground surface, and possibly harmfully impact water quality of near surface aquifers used for drinking water.

Nano particle has been successfully used for increasing the viscosity of CO_2 by generating foam in the porous media and therefore reducing the mobility of CO_2, however, the transport properties of the created emulsion in unknown.

Moreover, injectivity of CO_2 in depleted oil reservoir is lower than the absolute permeability of the repositories because of the residual oil. In this study we applied CT scanning techniques to measure the relative permeability and stability of the CO_2.

Research Objectives

Experiment

Use CT scanning to measure nano-particle concentration, and the different flow patterns caused by the foaming ability of nano-particles. Study the effect of nano particle in blocking the fracture in the carbonates rock.

Study the transport behavior of supercritical CO_2 during immiscible 3-phase displacement. Measuring the relative permeability and saturation routes of CO_2 at in CCS.

Theory

Developing three-phase relative permeability model for CCS.

Figure 1: Experimental set-up.
CO_2 is injected to the system from top of the column. We used fractured carbonate or sand stone core with 3" diameter and 2' long for the nano – particle enhanced foam and CO_2 flooding. During the scan, we controlled the index value (The distance between images) according to the injection velocity.

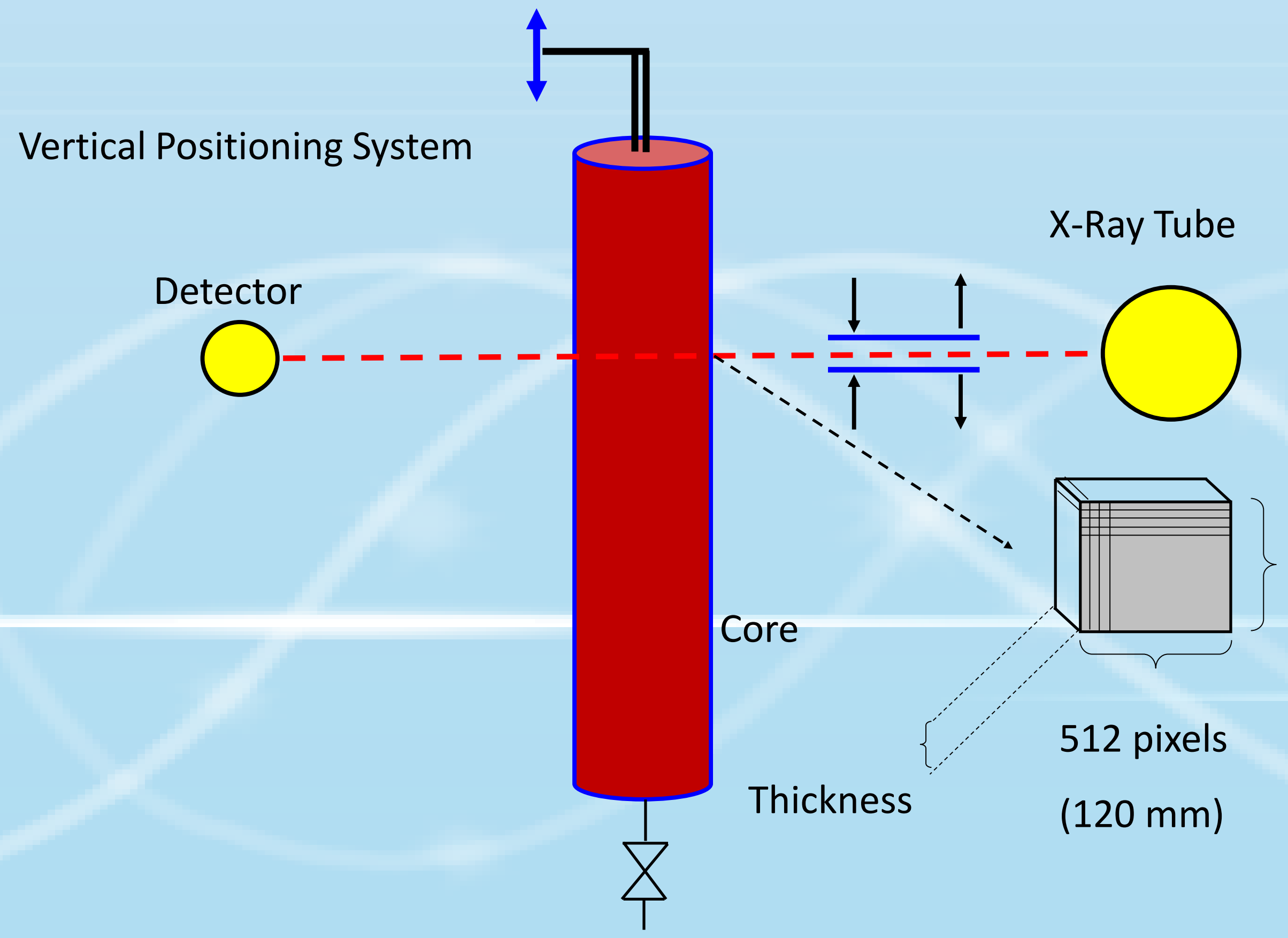

Experimental Research Plan

- Applying a new generation of CT scanner with vertical and horizontal capabilities and fast data acquisition time (4-6 seconds compared to 4 minutes)
- Obtaining relative permeabilities and saturation routes during 3-phase gravity drainage experiments
- Measuring 3-phase relative permeabilities and dynamic capillary pressure during immiscible CO_2 injection at high pressure
- Measuring the concentration of nano-particles in the emulsion that can be detected through CT scanning
- Measuring aperture in fractures using CT scanning
- Perform flow pattern experiments in recently acquired 3" core holder and fractured and unfractured cores

Experimental Results

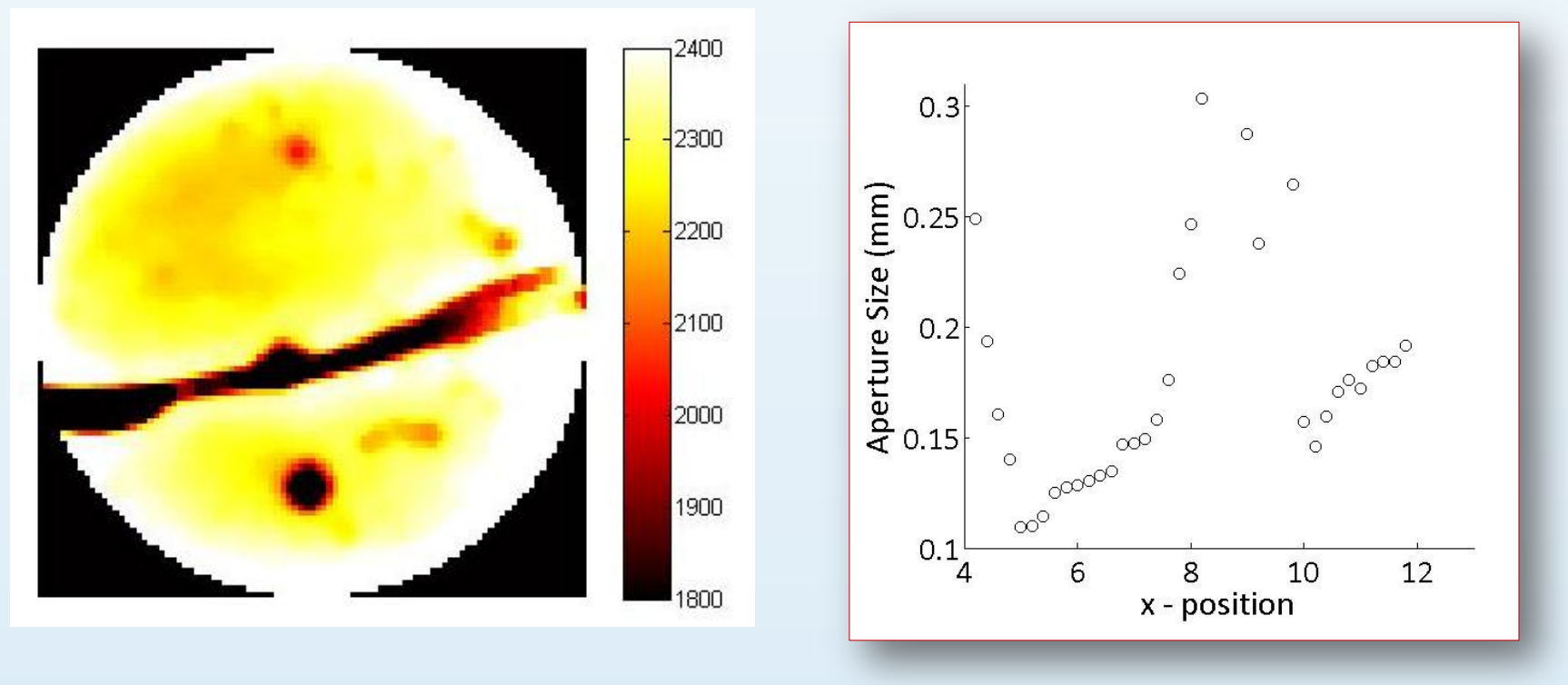

Figure 2: CT – image of a fractured core
One of the main aspect in developing the transport model of carbon dioxide in fractured rock is the fracture aperture. By using the CT scanning techniques we could successfully measure the fracture aperture in 3 dimension.

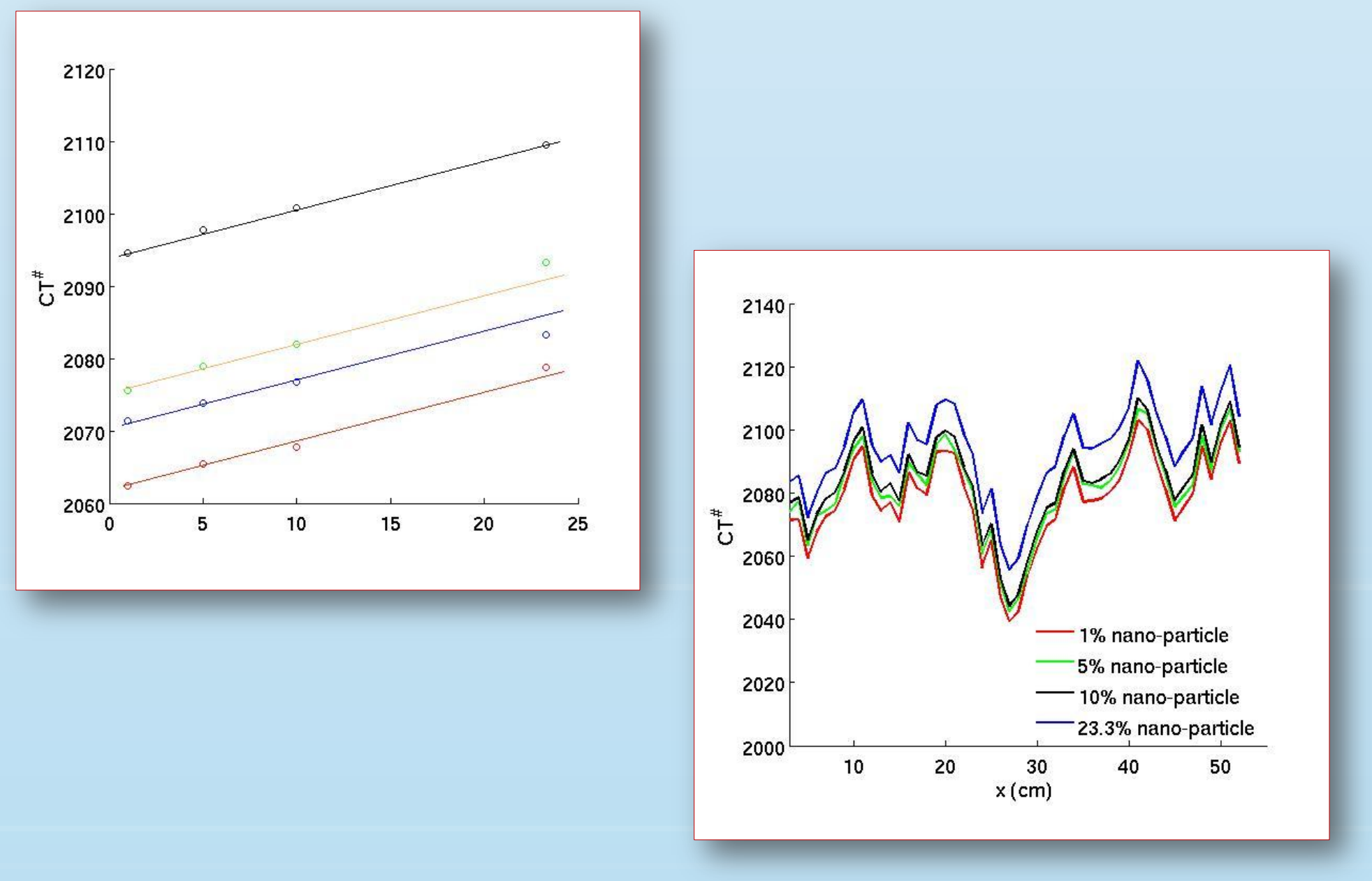

Figure 3: CT nano particle calibration curve
The main challenge in using CT scanner was to make nano – particle visible to the scanner, since the silica nano particle has the same density as the media (for sand stone rocks), as it shown in this figure by using the coating not only reduce the amount aggregation but also make them CT visible.

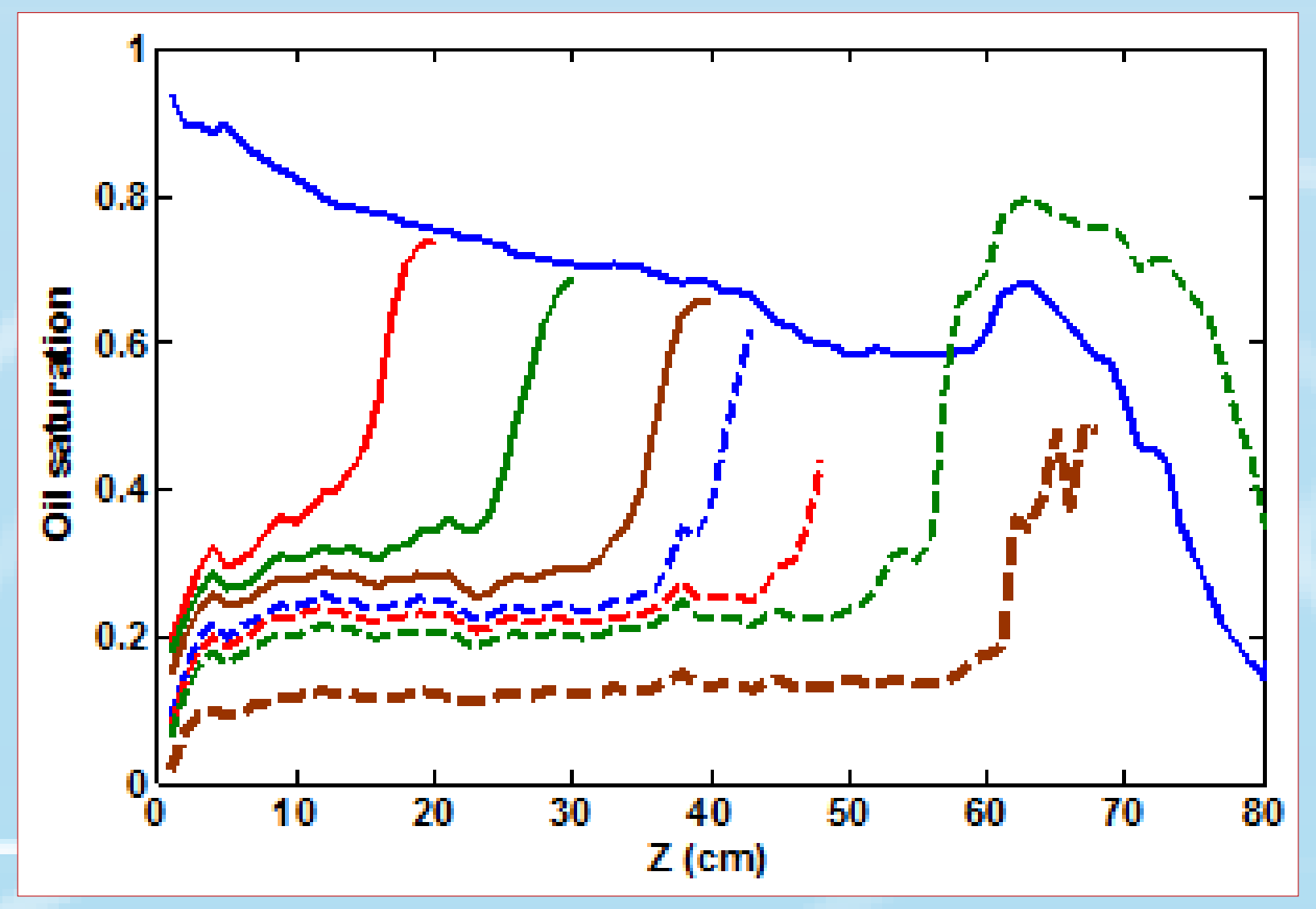

Figure 4: Saturation profile
By applying dual energy CT scanning techniques, we can measure the saturation profile for the 3 phase flow. This figure shows the saturation profile of the intermediate phase along the column at different times, and the solid blue curve shows the initial condition. During the CCS in the oil reservoir Co_2 would be the intermediate phase.

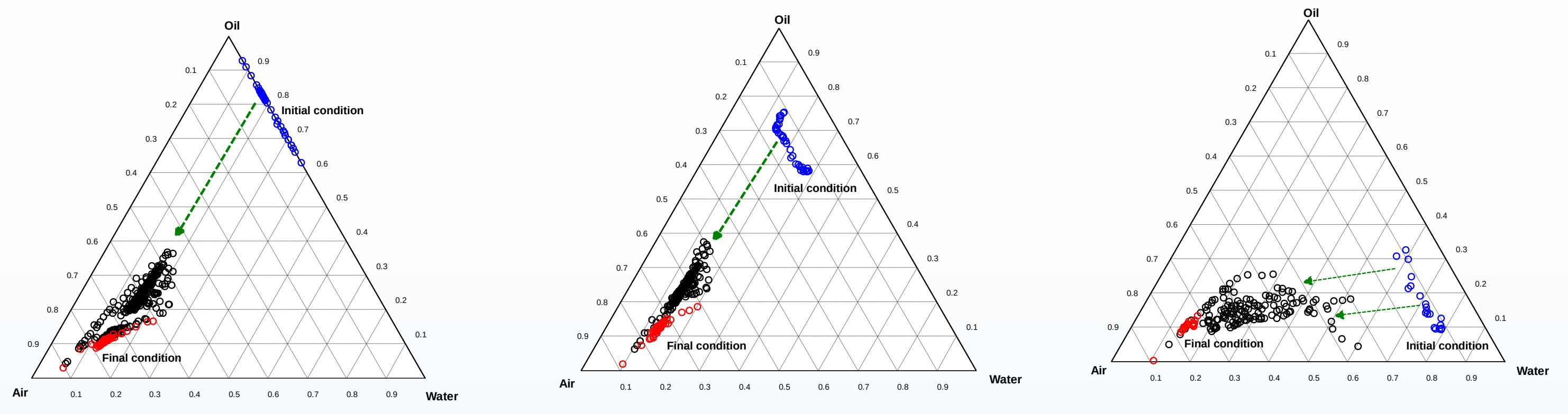

(a) (b) (c)

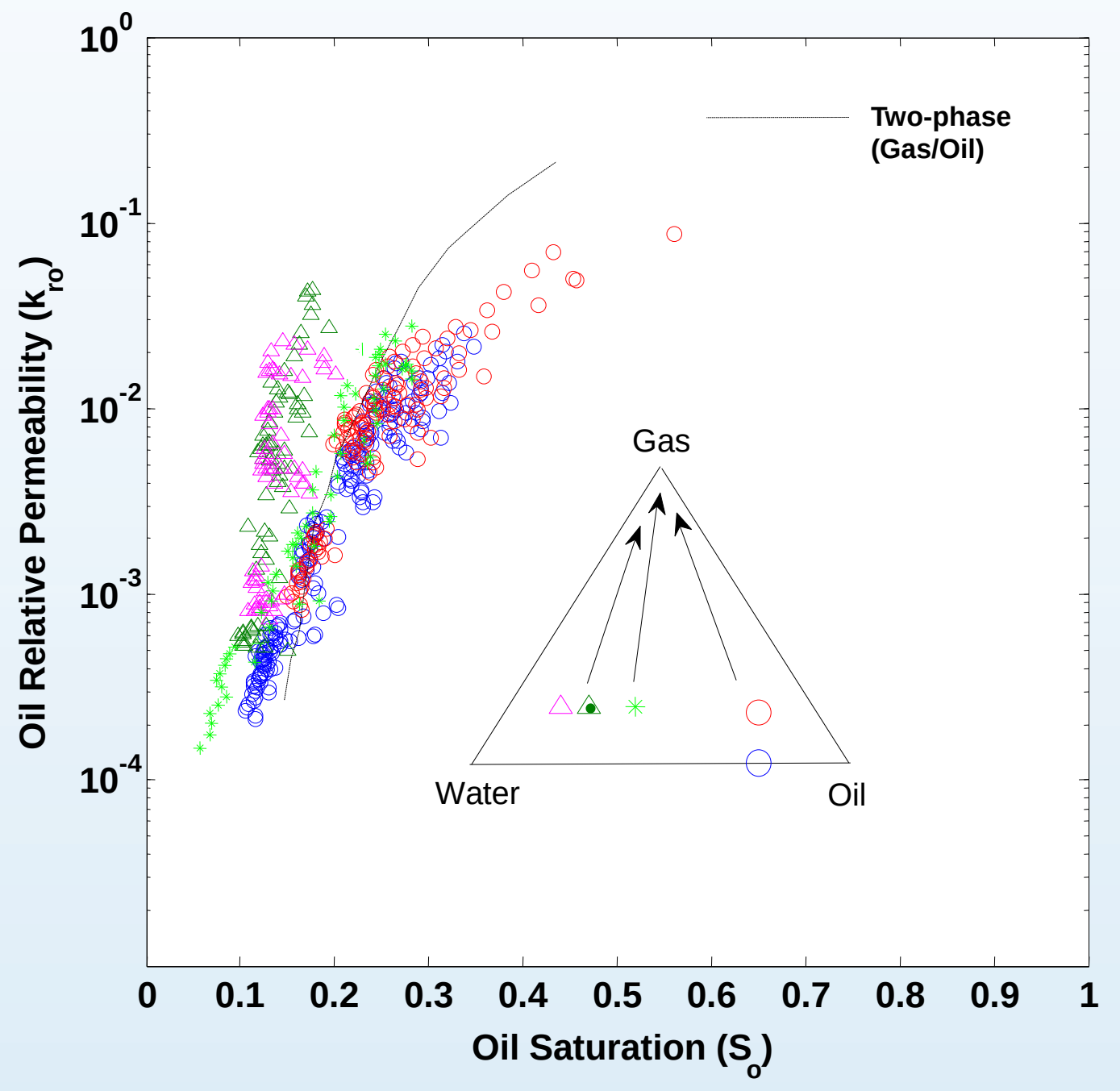

Figure 5: intermediate phase relative permeability measured during three-phase gravity drainage. The interesting observation is the measured k_{ro} data starting from residual oil (triangles), $S_o \approx 0.18$. Before the gas is allowed to invade, the oil is immobile and necessarily $k_{ro} = 0$, but when gas enters the column, k_{ro} jumps to $k_{ro} > 3*10^{-2}$. At 2-phase residual So ≈ 0.18, k_{ro} is two orders of magnitude greater than the measured k_{ro}^{2ph} and k_{ro} from tests starting at residual water saturation (circles).

Figure 6: the effect of viscosity ratio on intermediate layer conductance. We use the finite element method to solve the creeping flow approximation of Navier-Stokes equation (i.e., Poisson equation) for stable intermediate layers sandwiched between wetting water and gas in the center.

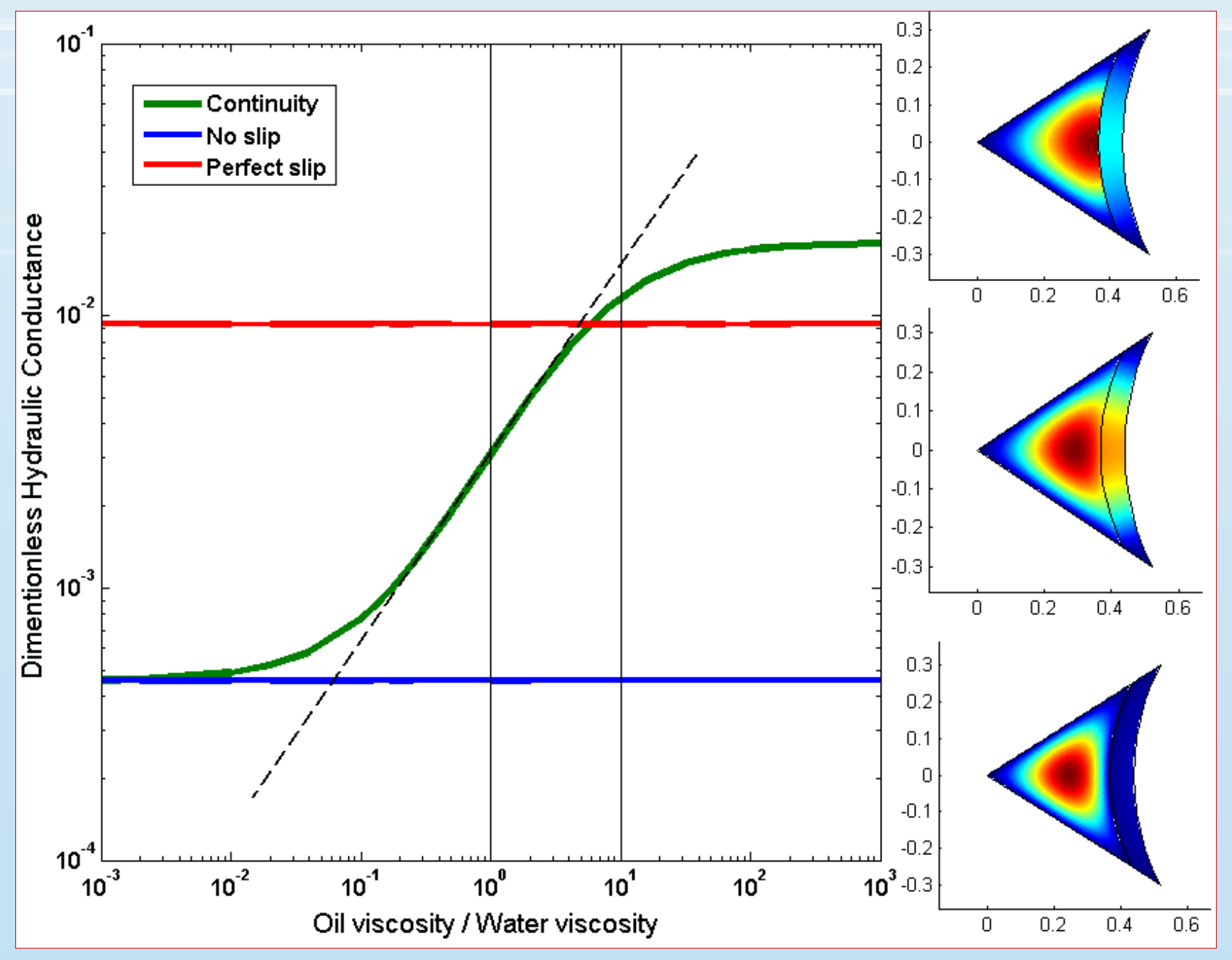

For this specific geometry, the hydraulic conductance is strongly correlated to the viscosity ratio when $0.1<\mu_o/\mu_w<10$. When $\mu_o/\mu_w>10$, the computed conductance is even higher than the values computed by assuming perfect slip boundary condition.

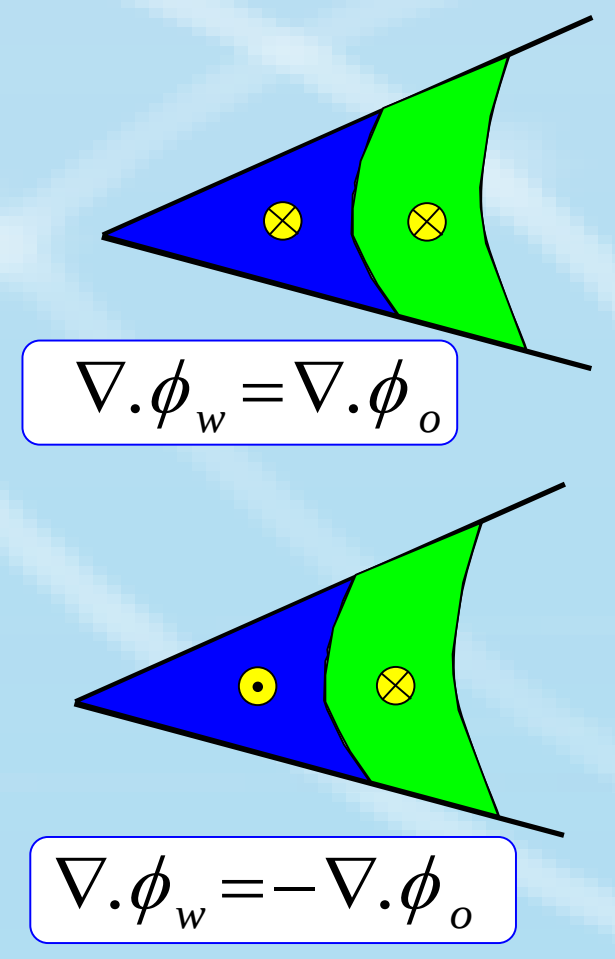

$\nabla.\phi_w = \nabla.\phi_o$

$\nabla.\phi_w = -\nabla.\phi_o$

$$\left.\begin{aligned}
&\nabla.(\tilde{\mu}\,\nabla.\vec{\tilde{V}}_o) = 1\\
&\nabla.(\nabla.\vec{\tilde{V}}_w) = 1\\
&\begin{pmatrix}\vec{\tilde{V}}_o\\ \vec{\tilde{V}}_w\end{pmatrix} = \begin{pmatrix}k_{oo} & k_{ow}\\ k_{wo} & k_{ww}\end{pmatrix}\begin{pmatrix}1/\tilde{\mu}\\ 1\end{pmatrix}\\
&\nabla.(\tilde{\mu}\,\nabla.\tilde{V}_o) = -1\\
&\nabla.(\nabla.\tilde{V}_w) = 1\\
&\begin{pmatrix}\tilde{V}_o\\ \tilde{V}_w\end{pmatrix} = \begin{pmatrix}k_{oo} & k_{ow}\\ k_{wo} & k_{ww}\end{pmatrix}\begin{pmatrix}-1/\tilde{\mu}\\ 1\end{pmatrix}
\end{aligned}\right\}
\begin{bmatrix}k_{oo}\\ k_{ow}\\ k_{wo}\\ k_{ww}\end{bmatrix} = \tilde{\mu}\begin{bmatrix}1 & \tilde{\mu} & 0 & 0\\ 0 & 0 & 1 & \tilde{\mu}\\ -1 & \tilde{\mu} & 0 & 0\\ 0 & 0 & -1 & \tilde{\mu}\end{bmatrix}^{-1}\begin{bmatrix}\vec{\tilde{V}}_o\\ \vec{\tilde{V}}_w\\ \tilde{V}_o\\ \tilde{V}_w\end{bmatrix}$$

$$\tilde{V}_w = V_w\left(\frac{\mu_w}{\nabla\phi_w k}\right),\quad \tilde{V}_o = V_o\left(\frac{\mu_w}{\nabla\phi_w k}\right),\quad \tilde{\mu} = \frac{\mu_o}{\mu_w}$$

Four independent coupled Darcy equations are obtained by solving Poisson equation for concurrent and countercurrent three-phase flow of oil and water in the cornet of the capillary.